Thermodynamics and mechanics of bilayer membranes

S. M. Oversteegen* and F. A. M. Leermakers
Laboratory of Physical Chemistry and Colloid Science, Wageningen University, P.O. Box 8038, 6700 EK Wageningen, The Netherlands
(Received 30 March 2000; revised manuscript received 20 June 2000)

A mean-field lattice model is applied to chain molecules for the study of surfactant systems. As an example, $C_{12}E_5$ surfactants, modeled as $C_{12}O(C_2O)_5$ chains, are forced into cylindrical and spherical shaped vesicles in a monomer solvent. These aggregates are used to obtain the rigidity constants of the bilayers as a function of the hydrophilicity of the surfactant's headgroup from both a thermodynamic and a mechanical route. Within the numerical accuracy, both routes are fully consistent. The magnitude and sign of the rigidity constants are interpreted to gain insight into features of the experimentally well-established phase diagram. It is concluded that the lattice model is a potentially valuable tool to help understand the generic phase behavior of surfactant systems.

PACS number(s): 87.16.Dg, 82.65.Dp

I. INTRODUCTION

In an aqueous environment, surfactants self-assemble into finite-sized aggregates if their concentration exceeds the so-called critical micellization concentration. The characteristic length scale of these aggregates, e.g., the radius of spherical or cylindrical micelles, is comparable to that of the surfactant molecules. The formation dynamics [1] and interfacial geometry [2] of the aggregates can be related to this common length scale. Here we will focus on bilayer membranes, in which a double sheet of surfactants separates two aqueous phases. The exterior of the sheet consists of the hydrophilic headgroups, whereas the interior is formed by the hydrophobic tails of the surfactants. The thickness of the membrane is comparable to the size of the constituting surfactant molecules. Bilayer systems are of interest for industrial applications, e.g., cleaning and catalysis, and in life sciences, e.g., as models for biomembranes.

The headgroups of the surfactants are hydrated on the one hand but also overlap to some extent with the conformationally disordered tails. Consequently, the conformational fluctuations within the various parts of the surfactant molecules are correlated. If the headgroups are well-hydrated, i.e., swollen, their relatively large headgroup area allows for a disorder of the tail region. Conversely, a collapsed headgroup induces more conformational order in the tails.

Bilayer membranes are also subject to collective, wavelike, thermal motions of the constituting surfactant molecules. These so-called undulations give rise to a conformational disorder on the level of the membrane. When two bilayers approach each other, the undulations are confined, which gives a loss of conformational entropy. This loss leads to a repulsive steric interaction between the bilayers. A low rigidity allows for large shape fluctuations of a membrane and yields a strong steric repulsion. This suggests that the contribution to the Helmholtz energy per unit area owing to undulations, f_u, is inversely proportional to the bending rigidity of the bilayer membrane. Introducing the bending modulus k_c, which is an energy typically of the order k_BT [3,4], dimensional analysis gives

$$f_u \propto \left(\frac{k_BT}{k_c}\right)^{\alpha} \frac{k_BT}{r^2}. \tag{1}$$

Here α is a numerical constant and r is the distance between two adjacent membranes. Indeed, Helfrich [5] showed that $\alpha=1$ and has been confirmed by others [1,4]. However, the proportionality constant is still disputed [6]. Depending on the magnitude of k_c, and the prefactor in Eq. (1), the repulsive undulation energy, Eq. (1), may overcome the attractive van der Waals energy $f_{\mathrm{vdW}} \propto -A/r^2$, where A is the Hamaker constant [1]. In those cases, the stability of bilayer membranes largely depends on the bending rigidity. Hence, it is of interest to determine k_c for these types of surfactant systems.

Another parameter of interest for the phase behavior of the surfactant layer is the saddle-splay modulus $\bar{k}$. If $\bar{k}$ is positive, the free energy of the interface can be lowered by forming saddle planes which have negative Gaussian curvatures K. It follows from the Gauss-Bonnet theorem [4,7]

$$\int K dA = 4\pi(1-g)$$

that g handles can be formed on a closed interface. For instance, $g=0$ for a spherical interface ($K=1/R^2$). Consequently, a positive saddle-splay modulus favors the formation of handles. Hence, $\bar{k}$ determines the topology of surfactant layers.

The phase behavior of surfactants can thus be understood in terms of the rigidity constants [8]. In order to study these constants k_c and $\bar{k}$ of a bilayer membrane, the free energy of the interface has to be considered as a function of curvature. This can best be done by considering closed bilayers or so-called vesicles. Vesicles are of interest for many biological purposes and are used as, e.g., drug delivery vehicles [1–3,7]. In the case of vesicles, there are no end-cap contributions to the free energy of the bilayer [2]. This also allows

*Present address: Van 't Hoff Laboratory for Physical and Colloid Chemistry, Debye Research Institute, Utrecht University, P.O. Box 80051, 3508 TB Utrecht, The Netherlands.

the application of a lattice model where spherically and cylindrically shaped structures can be studied.

In the present paper, we will consider the phase behavior of the nonionic surfactant dodecyl penta(ethylene oxide), or briefly $C_{12}E_5$. This nonionic surfactant can form vesicles and is widely used as an emulsifying agent and detergent. It exhibits the same characteristic features as more complex, multicomponent surfactant systems [9]. Consequently, much experimental data are available for this system [9,10]. First we will derive in Sec. II how the rigidity constants can be deduced consistently from both a thermodynamic and mechanical analysis. In order to study surfactants, a lattice model is briefly considered in Sec. III. Subsequently, in Sec. IV the rigidity constants of $C_{12}E_5$ vesicles will be investigated as a function of the hydrophilicity of the headgroup. From the obtained values, possible implications for the phase behavior will be discussed in Sec. V. Finally, recommendations for further study are given.

II. THERMODYNAMICS AND MECHANICS OF CURVED INTERFACES

In spite of the fact that we will focus in this paper on bilayer membranes in a single-component solvent, we first treat interfaces more generally, such that we need not go into detail about the structure of the interface. It will turn out that this generalized treatment, which originates from the early work of Gibbs [11] and Tolman [12,13], is easily applied to surfactant bilayers. Consider a two-phase system consisting of the bulk phases α and β. The interface between both phases is generally not sharp due to the thermal motion of the molecules. Consequently, there is no unambiguous position of the interface. Following Gibbs [11], the system is split up into two bulk phases separated by an infinitely thin interface at an arbitrary position R_s. The bulk values of the state variables are extrapolated up to the interface and the excesses are attributed to this arbitrary position [14]. Since we are interested in the mechanical work on a system, the grand potential is the appropriate state variable to study. For a two-phase system, the grand potential has proven to be [15]

$$\Omega=\Omega^{\alpha}+\Omega^{\beta}+\Omega^{s}=-p^{\alpha}V^{\alpha}-p^{\beta}V^{\beta}+\gamma A, \tag{2}$$

where p^b is the isotropic bulk pressure and V^b is the volume of the respective bulk phases $b=\alpha,\beta$. The curvature-dependent interfacial tension γ acts on the interfacial area A at the dividing plane located in R_s.

Mechanically, it is argued that the tangential pressure profile, $p_T(\vec{r})$, amounts to the grand potential [16]

$$\Omega=-\int p_T(\vec{r})d\vec{r}. \tag{3}$$

Upon comparison of the thermodynamic expression, Eq. (2), and the mechanical expression, Eq. (3), for the total grand potential, it is found that the excess pressure profile constitutes the grand potential of the interface,

$$\gamma A=\int_{V^{\alpha}}[p^{\alpha}-p_T(\vec{r})]d\vec{r}+\int_{V^{\beta}}[p^{\beta}-p_T(\vec{r})]d\vec{r}. \tag{4}$$

This relation holds for all geometries of the interface. In order to describe curved interfaces, we will use the so-called total curvature $J\equiv 1/R_1+1/R_2$ and Gaussian curvature $K\equiv 1/R_1R_2$, where R_1 and R_2 are the local radii of curvature of the interface at R_s. From the principle of parallel interfaces [17,18], the infinitesimal volume can be written as $d\vec{r}=A(R)dR$, where the interfacial area $A(R)$ at any position R can be given analytically relative to the interfacial area A at R_s [19]: $A(R)=A\{1+(R-R_s)J+(R-R_s)^2K\}$. Substitution of this into Eq. (4) and dividing by A gives

$$\gamma=\mathbb{P}_0+\mathbb{P}_1J+\mathbb{P}_2K, \tag{5}$$

where we introduced the zeroth, first, and second bending moments,

$$\mathbb{P}_0\equiv\int\{p^{\alpha\beta}-p_T(r)\}dR, \tag{6a}$$

$$\mathbb{P}_1\equiv\int(R-R_s)\{p^{\alpha\beta}-p_T(r)\}dR, \tag{6b}$$

$$\mathbb{P}_2\equiv\int(R-R_s)^2\{p^{\alpha\beta}-p_T(r)\}dR, \tag{6c}$$

where, in turn, the step function $p^{\alpha\beta}\equiv p^{\alpha}\theta(R_s-r)+p^{\beta}\theta(r-R_s)$ has been introduced, using the Heaviside step function $\theta(r)$. Note that the moments of the excess pressure profile $\mathbb{P}_0$, $\mathbb{P}_1$, and $\mathbb{P}_2$ depend on the arbitrary position of the interface, since $p^{\alpha\beta}$ generally depends on R_s.

We next consider the interfacial work needed to bend an interface. To that end, we use the well-known generalized Gibbs adsorption equation [15],

$$d\gamma=-\frac{S^s}{A}dT-\vec{\Gamma}\cdot d\vec{\mu}+\mathbb{C}_1dJ+\mathbb{C}_2dK, \tag{7}$$

where S^s is the interfacial entropy, T the temperature, $\vec{\Gamma}$ the adsorbed amount, and $\vec{\mu}$ the set of chemical potentials. The coefficients $\mathbb{C}_1$ and $\mathbb{C}_2$ conjugated to the curvature are the so-called bending stress and torsion stress, respectively [17]. Integration of Eq. (7) from the planar interface to an interface with a certain curvature (J, K) at constant temperature and chemical potentials yields for small deviations from the planar interface up to second order in the curvature

$$\gamma(J,K)\approx\gamma^0+\mathbb{C}_1^0J+\frac{1}{2}\left(\frac{\partial\mathbb{C}_1}{\partial J}\right)^0J^2+\mathbb{C}_2^0K, \tag{8}$$

where the superscript 0 denotes evaluation at the planar interface. Helfrich gave a similar expression for a phenomenological description of the undulation of lipid bilayers [20],

$$\gamma(J,K)=\gamma^0-k_cJ_0J+\tfrac{1}{2}k_cJ^2+\bar{k}K, \tag{9}$$

where J_0 is the spontaneous curvature. As argued in Sec. I, the saddle-splay modules $\bar{k}$ determines the topology of the interface rather than its rigidity, which is in turn determined by the bending modulus k_c. Comparison of Eq. (8) with the Helfrich equation, Eq. (9), yields the following thermodynamic expressions for the rigidity constants:

$$-k_c J_0 = \mathbb{C}_1^0 = \left(\frac{\partial \gamma}{\partial J}\right)^0_{T,\vec{\mu},K}, \tag{10a}$$

$$k_c = \left(\frac{\partial \mathbb{C}_1}{\partial J}\right)^0 = \left(\frac{\partial^2 \gamma}{\partial J^2}\right)^0_{T,\vec{\mu},K}, \tag{10b}$$

$$\overline{k} = \mathbb{C}_2^0 = \left(\frac{\partial \gamma}{\partial K}\right)^0_{T,\vec{\mu},J}, \tag{10c}$$

where we have used the well-known total differential Eq. (7) for the definitions of the bending and torsion stress. From the mechanical expression for γ, Eq. (5), we then find the following expressions for the rigidity constants in terms of the excess pressure profile:

$$-k_c J_0 = \mathbb{P}_1^0 + \left(\frac{\partial \mathbb{P}_0}{\partial J}\right)^0_{T,K}, \tag{11a}$$

$$k_c = 2\left(\frac{\partial \mathbb{P}_1}{\partial J}\right)^0_{T,K} + \left(\frac{\partial^2 \mathbb{P}_0}{\partial J^2}\right)^0_{T,K}, \tag{11b}$$

$$\overline{k} = \mathbb{P}_2^0 + \left(\frac{\partial \mathbb{P}_0}{\partial K}\right)^0_{T,J}. \tag{11c}$$

At first sight, all second terms on the right-hand sides of Eq. (11) are extra compared to the expressions given in the literature [3,21–24]; $-k_c J_0 = \mathbb{P}_1^0$, $k_c = (\partial \mathbb{P}_1 / \partial J)_{0,0}$, and $\overline{k} = \mathbb{P}_2^0$. Moreover, in the first term on the right-hand side of Eq. (11b), a factor 2 comes in compared to the literature. The extra terms make the thermodynamic variables independent of the choice of the expression for the local pressure [25]. Moreover, these terms require that one has to do real bending work; according to Eq. (11), evaluation of the planar interface only is no longer sufficient when the pressure is thermodynamically defined from Eq. (3).

Safran [3,21] derived mechanical expressions for the bending and saddle-splay moduli from virtual work. He assigned all the work to the pressure tensor, therefore the chemical potentials are embodied in the pressure, which is not consistent with the aforementioned thermodynamic definition that led to Eq. (11). Something similar occurs in the work of Szleifer *et al.* [26], where the pressure is strictly a Lagrange multiplier to satisfy packing constraints, which is not obviously the local pressure. Inserting this constraint into the partition function indeed adds a generalized pV term [22], also accounting for the chemical potentials. It has been shown indeed that the change in the chemical potentials must be accounted for in their expressions [27]. However, far above the critical micellization concentration, this change is negligible and for lower concentrations this can be corrected for by a normalization factor [21]. Gompper *et al.* [23] define a Ginzburg-Landau free-energy density as the excess pressure profile. It can be shown that in the vicinity of a critical point, the mechanical expressions from such a free-energy density numerically yield the same rigidity constants as Eq. (11) for simple liquid-vapor interfaces [28]. We conclude that distinction in the definitions for the local pressure explains the differences between Eq. (11) with those given in the literature. Somehow, the ''extra'' terms of Eq. (11) are incorporated in the previously mentioned pressures in the first terms for definitions of the local pressure other than from Eq. (3). Consequently, simply copying the expressions from the literature, as has been done in previous studies [29], may lead to incorrect results if the pressure has a different origin.

As may be clear from the above, it is necessary to apply a model in order to evaluate either of the equations (10) and (11). In the remainder of this paper, we will use a mean-field lattice model in which all conformations of chain molecules are accounted for. By constraining the molecules to the geometry of the lattice, we impose a curvature to the surfactant assemblies.

III. A LATTICE MODEL FOR SURFACTANT SOLUTIONS

We will apply a mean-field lattice model [30] to model the surfactant bilayer system, as elaborated before [29,31,32]. Here we will briefly summarize the relevant features of this generalized Flory-Huggins model. In order to have an easily accessible partition function, space is divided into cells with an equal volume of molecular size. The thus formed lattice consists of $z = 1, \ldots, M$ different layers, each containing $L(z)$ indistinguishable sites. In order to have all sites of equal volume v_0, the number of sites per layer depends on the geometry and the layer index z. That is, $L(z) \propto z^d$, where d is the dimensionality of the lattice ($d=0$ is a planar, $d=1$ a cylindrical, and $d=2$ a spherical lattice) [33]. The fractions of adjacent sites in each layer z, the so-called transition probabilities, are given by the parameters λ. The fraction $\lambda_0(z)$ is the probability of finding an adjacent site in the same layer z, whereas $\lambda_{-1}(z)$ and $\lambda_1(z)$ are the probabilities of finding adjacent sites in the previous and next layer, respectively. These are defined such that a detailed balance is satisfied. That is, the probability of finding an adjacent site in the next layer, $\lambda_1(z)L(z)$, is equal to the probability of finding an adjacent site in the previous layer relative to the next layer, $\lambda_{-1}(z+1)L(z+1)$ [33].

Before we can write down the grand potential, we first introduce the so-called contact fraction,

$$\langle \phi(z) \rangle \equiv \lambda_{-1}(z)\phi(z-1) + \lambda_0(z)\phi(z) + \lambda_1(z)\phi(z+1), \tag{12}$$

where $\phi(z)$ is the volume fraction of a species in layer z. From series expansion of $\phi(z-1)$ and $\phi(z+1)$, this may be approximated in continuous space as $\langle \phi(z) \rangle \approx \phi(z) + \lambda_1[(\partial^2\phi/\partial z^2) + (d/2)(\partial\phi/\partial z)]$, where d is again the dimensionality of the lattice and $\lambda_1 = \lim_{z\to\infty}\lambda_1(z)$.

Using the above contact fraction, the energy a segment of type A encounters at layer z is, relative to the bulk phase β, given by [32]

$$u_A(z) = u'(z) + k_B T \sum_B \chi_{AB}[\langle \phi_B(z) \rangle - \phi_B^\beta]. \tag{13}$$

Here ϕ_B is the volume fraction of all other segment types B. The energy $u'(z)$ comes in to account for the constraint that the lattice must be completely filled. The interactions between the segment types A and B are accounted for by the well-known Flory-Huggins interactions parameter χ_{AB}.

The volume fraction profiles of the various segments follow trivially from the corresponding volume fraction profiles of the molecules. The latter are found by generating all possible and allowed conformations of each molecule and are weighted by the appropriate Boltzmann factor. In this factor, the potential energy for a chain in a given conformation only depends on the potentials $u_A(z)$ experienced by the individual segments along the chain. In generating chain conformations, we have used a first-order Markov approximation. That is, chain connectivity is guaranteed but correlations along the chain between preceding and subsequent segments are ignored. Within this approximation, an efficient matrix procedure is available to generate the segment densities [30].

Hence, the volume fractions of the segments of type A follow from the energies $u_A(z)$ [30,32]. As can be seen from Eq. (13), the energies $u_A(z)$ depend, in turn, on the volume fractions. Consequently, the set of equations has to be solved iteratively until the energies and volume fraction are consistent.

The grand potential relative to its bulk value can be derived in terms of the volume fraction profiles from statistical thermodynamics [29,32],

$$\frac{\Omega+p^{\beta}V}{k_BT}=\sum_z L(z)\Bigg\{\sum_i \frac{\phi_i^{\beta}-\phi_i(z)}{N_i} -\sum_A \frac{\phi_A(z)u_A(z)}{k_BT}+\frac{1}{2}\sum_A\sum_B \chi_{AB}\{\phi_A(z) \times[\langle\phi_B(z)\rangle-\phi_B^{\beta}]-\phi_A^{\beta}[\phi_B(z)-\phi_B^{\beta}]\}\Bigg\} =\sum_z L(z)\{p^{\beta}-p_T(z)\}. \tag{14}$$

This defines the excess pressure profile, $p^{\beta}-p_T(z)$, in terms of the volume fractions. The factor $\frac{1}{2}$ of the third term in large curly brackets enters to correct for double-counting the interactions while summing over all species A and B. This means that the interactions between species A and B are effectively locally averaged over both species. However, one can also perform the double sum $\frac{1}{2}\Sigma_A\Sigma_B$ as $\Sigma_A\Sigma_{B>A}$, using the property that $\Sigma_z\phi_A(z)\langle\phi_B(z)\rangle=\Sigma_z\phi_B(z)\langle\phi_A(z)\rangle$. In this way, the interactions are assigned to only one of the species. Although both ways of counting the interactions yield the same grand potential, the excess pressure profile $p^{\beta}-p_T(z)$ is locally different. Still other schemes to calculate the double sum can be thought of, each yielding the same grand potential but different excess pressure profiles. Consequently, the local pressure is ambiguous, although it yields an unequivocal value for the grand potential [25].

IV. BENDING A BILAYER

A. Thermodynamics of bilayer membranes

As outlined in Sec. I, the rigidity of a bilayer determines the phase behavior of bilayer membranes to some extent. The rigidity constants can be derived from the curvature dependence of the interfacial tension, as expressed in the Helfrich equation, Eq. (9) [20]. Thermodynamically, the interfacial tension follows from [cf. Eq. (2)]

$$\Omega+p^{\beta}V=-\Delta pV^{\alpha}+\gamma A, \tag{15}$$

where A is the area of the bilayer and V^{α} the volume enclosed by the membrane. Since the inner bulk phase α, enclosed by the bilayer, is identical to the continuous outer phase β, there is no Laplace pressure drop, i.e., $\Delta p=0$. An equilibrium system of membranes that forms spontaneously from the surfactant solution can adapt its own number of bilayers with the corresponding interfacial area A. It follows from the thermodynamics of small systems [34–37] that for an equilibrium bilayer membrane, neglecting the translational entropy of the membrane, the equilibrium bilayer is tensionless, i.e., $\gamma=0$ [29]. Moreover, it is easily seen from symmetry considerations that the equilibrium membrane has on average a planar geometry [38], i.e., $J_0=0$. Hence, the Helfrich equation (9) for bilayer membranes reduces to

$$\frac{\Omega+p^{\beta}V}{A}=\gamma=\tfrac{1}{2}k_cJ^2+\overline{k}K. \tag{16}$$

B. Mechanics of bilayer membranes

It has been shown in Sec. II that the rigidity constants can also be obtained mechanically, i.e., in terms of the (excess) pressure profile. The bending modulus k_c and spontaneous curvature J_0 can be found directly from the cylindrical bilayer. The saddle-splay modulus $\overline{k}$ can only be determined from comparison of the bending modulus and the effective modulus of the spherical vesicle [cf. Eq. (11)],

$$-k_cJ_0=\mathbb{P}_1^{c,0}+\left(\frac{\partial\mathbb{P}_0^c}{\partial J}\right)_T^0, \tag{17a}$$

$$k_c=2\left(\frac{\partial\mathbb{P}_1^c}{\partial J}\right)_T^0+\left(\frac{\partial^2\mathbb{P}_0^c}{\partial J^2}\right)_T^0, \tag{17b}$$

$$k_c+\tfrac{1}{2}\overline{k}=2\left(\frac{\partial\mathbb{P}_1^s}{\partial J}\right)_T^0+\left(\frac{\partial^2\mathbb{P}_0^s}{\partial J^2}\right)_T^0+\tfrac{1}{2}\mathbb{P}_2^{s,0}, \tag{17c}$$

where the superscripts ''c'' and ''s'' refer to evaluation at the cylindrical and spherical interface, respectively. The bending moments, Eq. (6), for the lattice model are [28]

$$\mathbb{P}_0=\sum_{z=1}^{M}\{p^{\beta}-p_T(z)\}, \tag{18a}$$

$$\mathbb{P}_1=\sum_{z=1}^{M}(z-R_s-\tfrac{1}{2})\{p^{\beta}-p_T(z)\}, \tag{18b}$$

$$\mathbb{P}_2=\sum_{z=1}^{M}[(z-R_s)^2-(z-R_s-\tfrac{1}{3})]\{p^{\beta}-p_T(z)\}. \tag{18c}$$

The excess pressure profile $p^{\beta}-p_T(z)$ is given by Eq. (14). Moreover, because there is no Laplace pressure difference, we used that $p^{\alpha\beta}=p^{\beta}$ for bilayer membranes.

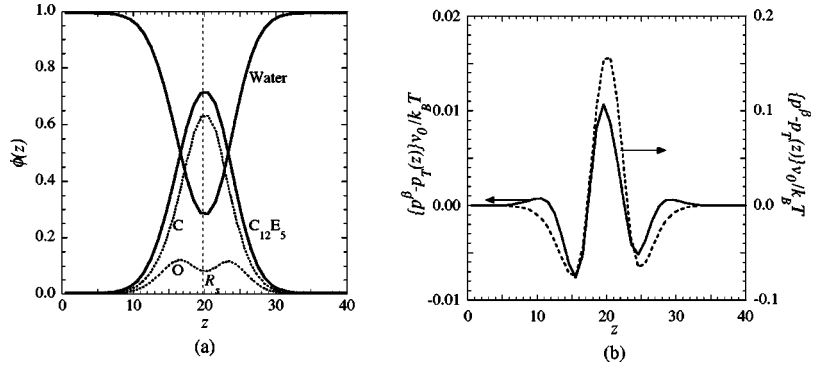

FIG. 1. (a) Volume fraction profiles of a cylindrical $C_{12}E_5$ vesicle in water. The surfactant $C_{12}E_5$ is modeled as $C_{12}O(C_2O)_5$, where the C represents CH_2 or CH_3 groups and the O mimics the O or OH groups. Water has been treated as a monomer with orientation-independent interactions. A lattice of 40 layers has been used with $\lambda_0=1/3$, $\chi_{CW}=\chi_{CO}=1.6$, and $\chi_{OW}=-0.5$. The dividing plane at R_s is chosen to be in the middle of the bilayer, whereas the center of the vesicle is located at $z=0$. (b) The tangential excess pressure profile corresponding to the density profiles as given in (a) can be determined in various ways yielding the same grand potential. The excess pressure represented by the solid line (left vertical axis) effectively averages the interactions with units in adjacent layers, whereas the dashed line (right vertical axis) one gives the excess pressure where the interactions with units in adjacent layers are assigned to one of the layers. Note that the scales differ by one order of magnitude.

C. Results for $C_{12}E_5$ in water

Using the lattice model, the $C_{12}E_5$ surfactants will be modeled as the chain molecule $C_{12}O(C_2O)_5$. Here, C stand for CH_2 or CH_3 groups, which will not be discriminated, and O mimics the oxygen or hydroxyl groups in the surfactant. The water molecules will be modeled by a simple monomer solvent *W*. Obviously, this is a poor model for water but can be improved by accounting for the orientation-dependent interactions in a quasichemical model [39]. Given the three monomer types *C*, *O*, and *W*, three exchange parameters χ_{CO}, χ_{CW}, and χ_{OW} need to be specified. Indicating that the interactions with the *C* group are hydrophobic, the exchange parameters are positive and are taken to be constant [31,40–42], $\chi_{CO}=\chi_{CW}=1.6$. However, owing to the hydration of the hydrophilic *O* groups by the water molecules, χ_{OW} is more strongly temperature-dependent. Consequently, varying χ_{OW} may be regarded as changing the temperature. Moreover, an fcc lattice type will be used, i.e., $\lambda_0=\lambda_1=\frac{1}{3}$. This lattice type in conjunction with the relatively low exchange parameters χ suppresses the so-called lattice artifact [29,43]. This artifact is originated in the fact that owing to the discretization of space, the fixed number of molecules are forced to take place in one layer or the other, i.e., they are ''squeezed'' onto the lattice. Consequently, an extra field is introduced as a result of the presence of the lattice, which causes a perturbation of the equilibrium state.

In order to determine the interfacial tension from the bending moments, Eq. (18) [cf. Eq. (5)], the position of the dividing plane R_s remains to be defined. Although both the inner and outer radius of the bilayer are possible choices, the dividing plane is found here from

$$\sum_{z=1}^{M}(z-R_s)\{\phi_s(z)-\phi_s^\beta\}=0, \tag{19}$$

where $\phi_s=\phi_C+\phi_O$ is the total surfactant volume fraction. The volume fraction profiles $\phi_C(z)$, $\phi_O(z)$, and $\phi_W(z)$ are illustrated in Fig. 1(a) for a cylindrical vesicle, where $\chi_{OW}=-0.5$ and the center of the vesicle is located at $z=0$ Using Eq. (19), the dividing plane is located to a good approximation in the middle of the membrane. The contributions to the *C* groups come from both the headgroups and the tails and are distributed over the complete bilayer. However, the *O* segments of the headgroups prefer the exterior of the vesicle but are relatively diffusively distributed because they are bound to the hydrophobic *C* groups. Note that the curved bilayer is asymmetric; the *O* groups are slightly more densely packed inside the vesicle ($z<R_s$) than the groups on the outside. This forces the tails outwards, hence the maximum of the *C* groups is found for $z>R_s$. Note the relatively large penetration of the monomeric water in the center of the membrane due to the lack of specific interactions. As stated before, this can be improved [39] but does not change the qualitative behavior of the present analysis.

Given the volume fractions, the excess pressure profile can be determined from Eq. (14). As stated, several ways to perform the double sum counting the nearest-neighbor interactions can be considered. Note the different features of the two examples given in Fig. 1(b). For instance, the range of the two given pressures differs by one order of magnitude, and the one given by the solid line has three maxima whereas the one given by the dashed line has only one. Nevertheless, both excess pressure profiles are slightly more tensile, i.e., negative, inside the vesicle than outside due to the curvature. The tensile parts are needed to compensate for the compressive, i.e., positive, parts resulting in the typical small interfacial tension.

With the above set of parameters and Eqs. (14) and (16), the rigidity constants can be determined from the curvature dependence of the interfacial tension as a function of the hydrophilicity χ_{OW} of the headgroup. The curvature of a bilayer is varied by changing the number of surfactants in the system. Given the number of surfactants, n_i, the constrained equilibrium density profiles are found. The equilibrium is constrained since the bilayer is forced into a curved, rather than a planar, geometry, which was shown to be the global equilibrium geometry. The resulting interfacial tensions are displayed by the symbols in Fig. 2(a) for both a spherical and cylindrical geometry as a function of the curvature taking

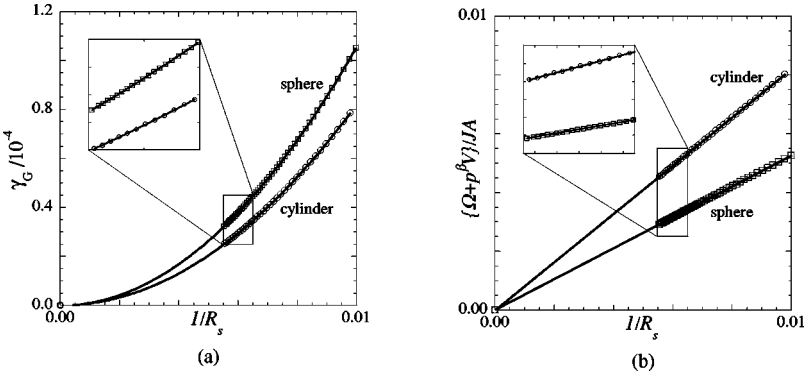

FIG. 2. (a) The interfacial tension of $C_{12}E_5$ bilayer membranes in water as a function of the curvature, with $\lambda_0=1/3$, $\chi_{CW}=\chi_{CO}=1.6$, and $\chi_{OW}=-0.5$. The position of the dividing plane is given by Eq. (19). The squares apply to a spherical vesicle, whereas the circles give the calculated values for a cylindrical geometry. The solid lines are a second-order polynomial fit to the points. (b) The linearized interfacial tension as given by Eq. (20) as a function of the curvature. The solid lines are linear fits to the calculated points. The magnifications show that the calculated values are subject to a relatively small lattice artifact.

$\chi_{OW}=-0.5$. A direct fit to the interfacial tension with a second-order polynomial, shown by the solid lines, yields according to Eq. (16) the rigidity constants. However, according to Eq. (16), the rigidity constants can also be found from a linear fit to

$$\frac{\Omega+p^\beta V}{JA}=\frac{\gamma}{J}=\begin{cases}\dfrac{1}{2}k_c\dfrac{1}{R_s} & \text{(cylinders)}\\ \left(k_c+\dfrac{1}{2}\overline{k}\right)\dfrac{1}{R_s} & \text{(spheres).}\end{cases} \tag{20}$$

The fit to Eq. (20) is shown in Fig. 2(b) for the same data. Using both the fit to γ and $(\Omega+p^\beta V)/JA$ gives information about the accuracy of the fits. Deviations may occur for two reasons. First, the calculated interfacial tensions are subject to lattice artifacts, as mentioned above. As can be seen from the magnifications in Fig. 2, the deviations from the fits are relatively small as expected for the given set of parameters. Second, the Helfrich equation is strictly only valid for small curvatures, i.e., $J\to 0$. However, as can most easily be seen from Fig. 2(b), the description remains appropriate for relatively large curvatures. Consequently, the curvature energy, $(\partial^2\gamma/\partial J^2)_T$, is hardly dependent on the curvature. This explains why vesicles, although not the equilibrium structure of the bilayer membranes, are relatively stable; the system can hardly change its free energy by growing or shrinking the vesicles. The system can only lower its free energy by fusing vesicles, which is an activated process. The average rigidity constants derived from Fig. 2 read $k_c=1.645\pm 0.002$ and $\overline{k}=-2.236\pm 0.002$. Apparently, the errors are relatively small. Since they are of a totally different origin, it is not likely that the two different types of errors cancel each other.

The rigidity constants can also be determined mechanically, as given by Eq. (17). The derivatives in Eq. (17) are subsequently determined from a second-order polynomial and linear fit to the zeroth and first bending moment, respectively. Although the results are independent of the choice of the pressure profile, one may prefer a certain choice for favorable numerical accuracy. As can be seen from Fig. 3, for $\chi_{OW}=-0.5$ these fits are fairly accurate and are hardly subject to lattice artifacts. Moreover, extrapolation to the planar interface $(1/R_s\to 0)$ shows that $\mathbb{P}_0^{s,0}=\mathbb{P}_0^{c,0}=0$, which recovers the fact that the planar interface is tensionless if the translational entropy is neglected, as is the case in this study.

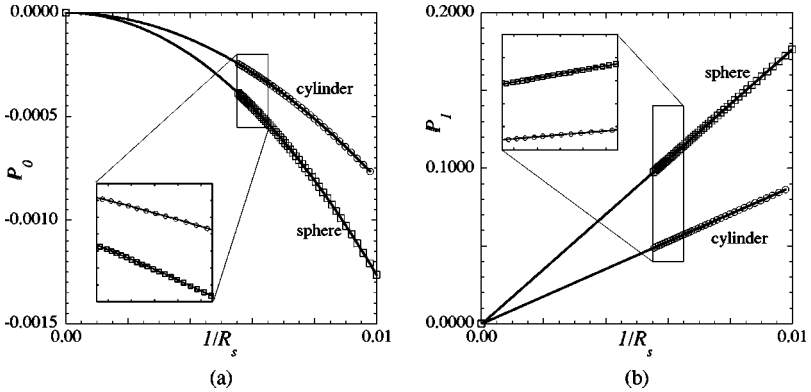

FIG. 3. (a) The zeroth bending moment of $C_{12}E_5$ bilayer membranes in water as a function of the curvature, with $\lambda_0=1/3$, $\chi_{CW}=\chi_{CO}=1.6$, and $\chi_{OW}=-0.5$. The position of the dividing plane is given by Eq. (19). The squares refer to a spherical vesicle, whereas the circles give the calculated values for a cylindrical geometry. The solid lines are a second-order polynomial fit to the points. The graph recovers the analytical result that the planar membrane is tensionless; $\gamma^0=\mathbb{P}_0^0=0$. (b) The first bending moment as a function of the curvature. The solid lines are linear fits to the calculated points. As expected from symmetry considerations, $\mathbb{P}_1^0=0$. The magnifications show that the calculated values are subject to a relatively small lattice artifact.

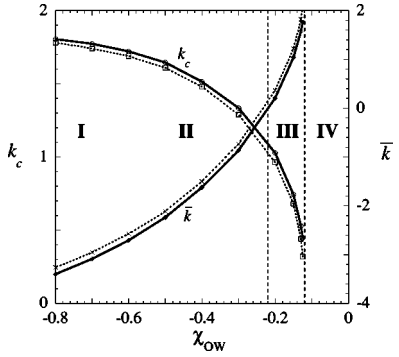

FIG. 4. The bending modulus and saddle-splay modulus for a $C_{12}E_5$ bilayer membrane as a function of the hydrophilicity of the headgroup with $\chi_{CO}=\chi_{CW}=1.6$, $\lambda_0=\frac{1}{3}$. The dividing plane is chosen to be in the middle of the membrane, using Eq. (19). The roman numbers indicate different phase regions.

Since the planar bilayer is completely symmetrical with respect to its center [cf. Eq. (19)], extrapolation indeed yields $\mathbb{P}_1^{s,0}=\mathbb{P}_1^{c,0}=0$. Furthermore, it is found that for the system as shown in Fig. 3, $\mathbb{P}_2^{s,0}=\mathbb{P}_2^{c,0}=-21.536$.

From the fits to the bending moments in Fig. 3, using Eq. (17), it is found that $J_0=0.00$, $k_c=1.61$, and $\bar{k}=-2.11$. The exact error in these values is unknown; the accuracy of the fits is hard to determine and the sum of the respective derivatives typically yields a number that is one order of magnitude smaller than the individual values. Otherwise stated, the discrepancies between the values for the rigidity constants determined from the direct fit to the interfacial tension and those determined from the bending moments are due to numerical errors.

The above procedure has been repeated for several values of χ_{OW}. The results for the bending modulus and saddle-splay modulus are shown in Fig. 4. The solid lines connect the symbols calculated from the direct fits to the interfacial tension. The error bars are smaller than the symbols. The dotted lines connect the symbols determined mechanically from the bending moments. There appears to be a constant, minor deviation between the mechanically determined rigidity constants and those determined from the fit to γ. This is due to the fact that the error in the fits to the bending moments is systematic. This apparently leads to the conclusion that the value for the mechanically determined bending modulus is typically too low. Consequently, since the sum must yield by definition the same interfacial tensions as those from the direct fit to γ, the saddle-splay modulus from the bending moments is slightly overestimated.

V. DISCUSSION AND CONCLUSIONS

Rigidity constants have been determined consistently from both a thermodynamic and mechanical route as a function of the hydrophilicity of the headgroup, which is closely related to the system's temperature. Different regions may be distinguished in Fig. 4. For $\chi_{OW}\lesssim -0.8$, the value of k_c is almost constant and relatively high. Owing to the relatively good solubility of the O groups, the headgroups are well-hydrated. Consequently, the hydrophobic tails of the surfactants are forced more inwards into the bilayer, as outlined in Sec. I. As a result, the membrane remains relatively rigid.

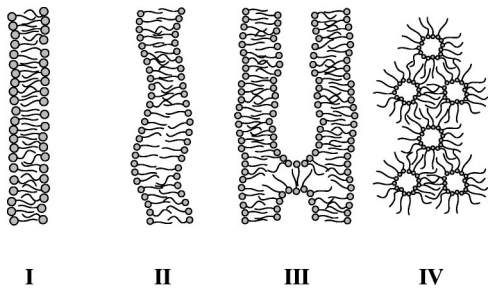

FIG. 5. Different phases can be observed from the calculations for $C_{12}E_5$ vesicles. I: For $\chi_{OW}\lesssim -0.8$, the $C_{12}E_5$ membranes are relatively rigid. II: For $-0.8\lesssim\chi_{OW}\lesssim -0.22$, k_c decreases, causing the bilayer to be less stiff, and yields an increasing spacing between the membranes. III: For $-0.22<\chi_{OW}<-0.12$, $\bar{k}$ becomes positive, which favors the formation of connecting handles between the bilayers. IV: If $\chi_{OW}\gtrsim -0.12$, the headgroups are not hydrophilic enough, such that the bilayers are unstable and the surfactants phase separates into a phase of inverted micelles.

Going through the range $-0.8\lesssim\chi_{OW}\lesssim -0.22$, the hydrophilicity decreases such that the headgroups can dissolve easier in the hydrophobic core of the membrane, making the membrane less rigid. Consequently, the values of the bending modulus decrease. Hence, the undulations increase with increasing χ_{OW}. As can be seen from Eq. (1), the repulsive forces in the system increase, which makes the spacing r between bilayer sheets larger. This correlates well with the experimental finding that the so-called L_α phase swells with increasing T [9,10].

For $-0.22<\chi_{OW}<-0.12$, the saddle-splay modulus becomes positive, which favors the formation of saddle planes. Consequently, although the low value of the bending modulus gives rise to a large repulsive force between the membrane sheets, connecting handles are formed between the bilayers. This may explain the experimentally observed L_3 or sponge phase at relatively high temperature [9].

If $\chi_{OW}\gtrsim -0.12$, the bending modulus tends to become negative and, like the saddle-splay modulus, even seems to diverge. This implies that the bilayer membranes are no longer stable. Moreover, the solubility of the headgroup has become so low that the system will phase-separate into an aqueous and a surfactant-rich phase. Since the O and C groups still repel each other, the surfactant molecules tend to form inverted micelles in which small amounts of water are dissolved. Such phases have indeed been observed experimentally at high temperatures [9].

The described phase behavior is summarized and illustrated schematically in Fig. 5 for the regions indicated in Fig. 4. Since all these phases have been observed experimentally for the $C_{12}E_5$ surfactant system in water [9,10], it is concluded that the lattice model is suitable for a qualitative study of the phase behavior of surfactant systems. Already with a restricted set of parameters, the basic experimental features of the phase diagram can be recovered. In order to do so, vesicles were forced into a cylindrical and spherical geometry, thus neglecting the end-cap energy and translation entropy of the actual bilayer membranes. From these vesicles, two independent fits to the interfacial tension yield consistent values for the rigidity constants of the surfactant bilayer membrane as a function of the hydrophilicity of the

headgroup. The values are recovered with less numerical accuracy from the mechanical expressions for the rigidity constants. Consequently, a direct fit to the interfacial tension suffices for future studies. It should be noted that the terms that appear extra in the mechanical expressions, Eq. (11), as compared to those in the literature due to the definition of the pressure, are required to amount to the same Helfrich constants for any choice of the pressure profile [cf. Fig. 1(b)]. Hence, these terms, which arise naturally in the analysis, are needed to guarantee consistency between the thermodynamic and mechanical route.

From the sign and magnitude of the bending and saddle-splay modulus, one can determine in what phase the surfactant layer prefers to be when the geometry restrictions are relaxed. Hence, minimal surfaces may be studied from cylindrical and spherical interfaces only. Nevertheless, the balance between attractive and repulsive forces accounting for the translational entropy of the bilayers upon actual inclusion of multiple membrane sheets in the calculations remains of interest. Incorporation of the influence of charges in ionic surfactant systems [44,45] and the role of, e.g., a cosurfactant or cosolvent on the phase behavior of surfactant layers is also a challenge for future study. Moreover, the phase behavior of surfactant monolayers, such as e.g., in microemulsions [46], as a function of the aforementioned parameters deserves profound attention.

It has been argued that the bending route to the rigidity constants, as elaborated on here, may lead to different rigidity constants and, by that, different phase behavior as compared to the fluctuation route [47]. This may be due to the fact that the undulations on the closed interface of the vesicle are subject to boundary conditions, which makes the number of waves quantized (cf. the ''particle in a box'' from quantum mechanics). This restriction introduces another entropic term that is not accounted for in the above route to the rigidity constants [48,49]. It is also of interest to study the influence of this kind of entropy on the differences in rigidity constants.

In the model for surfactant bilayers presented here, contributions of a lattice artifact have been shown to be negligible. However, in the previously recommended systems, this artifact may need attention. In the case of microemulsions, the amount of oil may be adjusted until the spurious Laplace pressure difference due to the artifact is eliminated. Since the enclosed phase equals the outer phase, this method is not applicable to vesicle systems. In a previous study [29], the number of surfactants of a vesicle system was adjusted until $\mathbb{P}_0=0$. As can be seen from Eq. (17), this implies that $\overline{k}=\mathbb{P}_2^0$, as had been found indeed. However, the condition $\gamma=\mathbb{P}_0=0$ only holds for the planar equilibrium membrane. This method thus appeared to eliminate the artifact by introducing one. Consequently, at present there is no longer a condition available to warrant artifact-free vesicles within the presented mean-field lattice model. Since the sign and the order of magnitude rather than the exact value of the rigidity constants determines the phase behavior, the lattice model may still prove to be a very valuable tool for the study of surfactant systems.

ACKNOWLEDGMENT

The work of S.M.O. was supported by the Netherlands Organization for Scientific Research Chemical Sciences (NWO/CW).

[1] D. Evans and H. Wennerström, *The Colloidal Domain: Where Physics, Chemistry, Biology and Technology Meet* (VCH Publishers, New York, 1994).
[2] J. Israelachvili, *Intermolecular and Surface Forces*, 2nd ed. (Academic Press, London, 1991).
[3] S. Safran, in *Frontiers in Physics*, edited by D. Pines (Addison-Wesley, Reading, MA, 1994), Vol. 90.
[4] D. Sornette and N. Ostrowsky, in *Micelles, Membranes, Microemulsions and Monolayers*, edited by W. Gelbart, A. Ben-Shaul, and D. Roux (Springer, Berlin, 1994), Chap. 5.
[5] W. Helfrich, Z. Naturforsch. A **33a**, 305 (1978).
[6] W. Helfrich, in *Liquids at Interfaces*, Les Houches, edited by J. Charvolin, J. Joanny, and J. Zinn-Justin (Elsevier, Amsterdam, 1990), Vol. XLVIII.
[7] S. Hyde *et al.*, *The Language of Shape: The Role of Curvature in Condensed Matter Physics, Chemistry and Biology* (Elsevier, Amsterdam, 1997).
[8] D. Morse, Curr. Opin. Colloid Interface Sci. **2**, 365 (1997).
[9] R. Strey *et al.*, J. Chem. Soc., Faraday Trans. **86**, 2253 (1990).
[10] D. Mitchell *et al.*, J. Chem. Soc., Faraday Trans. 1 **79**, 975 (1983).
[11] J. Gibbs, *The Scientific Papers* (OxBow Press, Woodbridge, 1993), Vol. 1, pp. 225–229.
[12] R. Tolman, J. Chem. Phys. **16**, 758 (1948).
[13] R. Tolman, J. Chem. Phys. **17**, 333 (1949).
[14] C. Reid, *Chemical Thermodynamics* (McGraw-Hill, Singapore, 1990).
[15] S. Oversteegen *et al.*, Phys. Chem. Chem. Phys. **1**, 4987 (1999).
[16] F. Buff, J. Chem. Phys. **23**, 419 (1955).
[17] C. Murphy, Ph.D. thesis, University of Minnesota, 1966.
[18] J. Gaydos *et al.*, in *Applied Surface Thermodynamics*, edited by A. Neumann and J. Spelt (Marcel Dekker, New York, 1996), Vol. 64.
[19] V. Markin, M. Kozlov, and S. Leikin, J. Chem. Soc., Faraday Trans. 2 **84**, 1149 (1988).
[20] W. Helfrich, Z. Naturforsch. C **28c**, 693 (1973).
[21] S. Safran, Adv. Phys. **48**, 395 (1999).
[22] A. Ben-Shaul and W. Gelbart, in *Micelles, Membranes, Microemulsions and Monolayers*, edited by W. Gelbart, A. Ben-Shaul, and D. Roux (Springer, Berlin, 1994).
[23] G. Gompper and S. Zschocke, Phys. Rev. A **46**, 4836 (1992).
[24] E. Blokhuis and D. Bedeaux, Heterog. Chem. Rev. **1**, 55 (1994).
[25] S. Oversteegen, P. Barneveld, F. Leermakers, and J. Lyklema, Langmuir **15**, 8609 (1999).
[26] I. Szleifer *et al.*, J. Chem. Phys. **92**, 6800 (1990).
[27] E. Blokhuis, H. Lekkerkerker, and I. Szleifer, J. Chem. Phys. **112**, 6023 (2000).
[28] S. Oversteegen and E. Blokhuis, J. Chem. Phys. **112**, 2980 (2000).

[29] P. Barneveld, J. Scheutjens, and J. Lyklema, Langmuir **8**, 3122 (1992).
[30] G. Fleer *et al.*, *Polymers at Interfaces* (Chapman and Hall, London, 1993).
[31] F. Leermakers and J. Scheutjens, J. Colloid Interface Sci. **136**, 231 (1990).
[32] O. Evers, J. Scheutjens, and G. Fleer, Macromolecules **23**, 5221 (1990).
[33] P. van der Schoot and F. Leermakers, Macromolecules **21**, 1876 (1988).
[34] T. Hill, *Thermodynamics of Small Systems* (W.A. Benjamin, New York, 1963), Vol. I (reprinted by Dover, Mineola, NY, 1994).
[35] T. Hill, *Thermodynamics of Small Systems* (W.A. Benjamin, New York, 1964), Vol. II (reprinted by Dover, Mineola, NY, 1994).
[36] D. Hall and B. Pethica, in *Nonionic Surfactants*, edited by M. Schick (Marcel Dekker, New York, 1967), Vol. 1, Chap. 16.
[37] D. Hall, in *Nonionic Surfactants; Physical Chemistry*, edited by M. Schick (Marcel Dekker, New York, 1987), Vol. 23, Chap. 5.
[38] D. Roux, C. Safinya, and F. Nallet, in *Micelles, Membranes, Microemulsions and Monolayers*, edited by W. Gelbart, A. Ben-Shaul, and D. Roux (Springer, Berlin, 1994), Chap. 6.
[39] N. Besseling and J. Lyklema, J. Phys. Chem. **98**, 610 (1994).
[40] P. Privalov and J. Stanley, Pure Appl. Chem. **61**, 1097 (1989).
[41] C. Tanford, *The Hydrophobic Effect: Formation of Micelles and Biological Membranes* (Wiley, New York, 1980).
[42] N. Besseling and J. Lyklema, J. Phys. Chem. B **101**, 7604 (1997).
[43] S. Oversteegen, Ph.D. thesis, Wageningen University, 2000 (unpublished).
[44] P. Barneveld *et al.*, Langmuir **10**, 1084 (1994).
[45] H. Lekkerkerker, Physica A **159**, 319 (1989).
[46] F. Leermakers *et al.*, Faraday Discuss. **104**, 317 (1996).
[47] E. Blokhuis, J. Groenewold, and D. Bedeaux, Mol. Phys. **96**, 397 (1999).
[48] W. Kegel and H. Reiss, Ber. Bunsenges. Phys. Chem. **100**, 300 (1996).
[49] W. Kegel and H. Reiss, Ber. Bunsenges. Phys. Chem. **101**, 1963 (1997).